

Theory of scanning tunneling microscopy of the (110) surface of GaAs based on the method of quasistationary states and the formalism of tight binding

S. N. Molotkov, S. S. Nazin, I. S. Smirnova, and V. V. Tatarskii

Institute of Solid State Physics, Russian Academy of Sciences

(Submitted 18 March 1992)

Zh. Eksp. Teor. Fiz. **102**, 1303–1314 (October 1992)

A model is proposed to interpret scanning tunneling microscopy (STM) images of the reconstructed (110) surface of GaAs. The model, which is based on the concept of quasistationary states and the tight-binding formalism, is used to calculate the STM images. The results obtained are found to be in good qualitative agreement with the experimental data.

1. INTRODUCTION

The discovery of scanning tunneling microscopy (STM) has made possible the study of surfaces at the atomic level.^{1–5}

The usual starting point for interpreting STM experiments is the Bardeen– Tersoff– Hamann theory^{6,7} for the tunneling current between two weakly coupled systems. In this approach, the current is given by the expression

$$I = \frac{2\pi e}{\hbar} \sum_{\mu, \nu} |T_{\mu\nu}|^2 \delta(\epsilon_\mu - \epsilon_\nu) [n(\epsilon_\mu) - n(\epsilon_\nu)], \quad (1)$$

where the Bardeen tunneling matrix element can be written in the form⁶

$$T_{\mu\nu} = \frac{\hbar^2}{2m} \int ds (\Psi_\mu \nabla \Psi_\nu^* - \Psi_\nu \nabla \Psi_\mu^*). \quad (2)$$

In Eq. (2) the integration is carried out over any surface that passes between the crystal and the tip, m is the free electron mass, Ψ_μ and Ψ_ν are unperturbed wave functions for states of the tip and the crystal, and ϵ_μ , ϵ_ν are the energy levels corresponding to these states.

Equation (1) is still not sufficient to provide a simple understanding of the atomic resolution in STM. Further progress in this direction was made in the work of Tersoff and Hamann⁷ and Baratoff,⁸ where it was proposed that the sharp point be modeled as a sphere of radius R . In the limit $R \rightarrow 0$ such tips turn into point test atoms whose wave functions are localized and have s -type symmetry. For small applied voltages, the expression for the tunneling current in this limit can be written in the form

$$I \propto \sum_c |\Psi_c(\mathbf{r}_0)|^2 \delta(\epsilon_c - \epsilon_f). \quad (3)$$

The derivation of Eq. (3) assumes that the tip is metallic, that ϵ_f is the Fermi energy in the tip, and that \mathbf{r}_0 is the location of the test atom (in the limit $R \rightarrow 0$). It follows from Eq. (3) that the tunneling current is proportional to the local density of states calculated at the point \mathbf{r}_0 , i.e., at the “tail” of the crystal wave function.

Thus, in the constant tunneling current regime, STM images correspond to contours of constant electron density near the crystal.

For the case of simple metals the spatial distribution of electronic states follows the geometric position of the atoms. For metals, STM usually gives the real topographical image of the surface. For semiconductors the electronic states do not follow the direct topographical contour. In this case in-

terpretation of an STM image is a nontrivial problem, requiring knowledge of the interrelationship of the electronic and atomic surfaces (i.e., the geometric structure of the surface).

Despite the apparent simplicity and transparency of Eq. (3), this approach suffers from important deficiencies. First of all, the atomic structure of the sharp point drops out of the discussion. A second and more serious deficiency was identified in the detailed and accurate analysis given in the paper by Chen⁹ of the original expression (1) and the transition from it to Eq. (3). Reference 9 showed that Eq. (3) is correct, and in fact independent of the atomic and electronic structure of the sharp point, only in the macroscopic limit, i.e., when the spatial scale of modulation of the electron density at the surface of the crystal greatly exceeds the atomic scale. In the opposite case, which is characteristic of the experimental situation, interpretation of STM images with atomic resolution using Eq. (3) becomes problematical. We also note that for simple metals, Eq. (3) gives a value of the profile modulation that is several times smaller than what is observed experimentally when the electron structure of the sharp point is ignored (see the analysis of the experimental data in Ref. 10). The authors of Refs. 9–11 attempted to take into account the electronic structure of the sharp point by including impurity states with other than s -like symmetries. Their generalization of Eq. (3) to include p - and d -orbitals of the sharp point improved the agreement with experiment.

It is clear from the derivation of Eq. (3) that effects due to the interaction between the tip and the crystal surface have been ignored. For small tunneling gaps these effects can turn out to be considerable. Attempts to include, e.g., changes in the surface spectrum (surface states induced by the tip for a fixed atomic geometry of the surface) were made by Tekman and Ciraci.¹² They used the Bardeen approach and the tight-binding method to study the effect of the next correction to the tunneling matrix element on the current. In what follows we will show that the effect of the tip-crystal interaction on the change in the spectrum can be included within the framework of tight binding in a systematic way.

2. THE TIGHT-BINDING METHOD IN THE THEORY OF STM

In this section we introduce some necessary information regarding the tight-binding method and its application to STM.

In recent years the method of tight binding has been used successfully to describe the properties of solids both in bulk and at a surface (see, e.g., the book by Harrison¹³ and

citations in it). The tight-binding method is not numbered among the so-called first-principles methods (although the fact is that these latter methods cannot avoid the use of fitting parameters of one sort or another). In tight-binding calculations the energy spectrum of the solid is described by a Hamiltonian in which overlap integrals are introduced between orbitals of various symmetries that are centered on atoms. As a rule it is sufficient to include overlap integrals between nearest neighbors. A large number of calculations of various properties of solids using this method have demonstrated¹³ that the matrix elements possess the property of transferability, i.e., matrix elements determined for one material (e.g., fitted to experiment) can be used for other materials. Of course, in this case it is necessary to include their dependence on bond length, which turns out to be quite universal, and within the range of variation of bond lengths in solids is well-described by the dependence $1/d^2$ (where d is the bond length).¹³ However, the angular dependence of the matrix elements is dictated by the symmetry of the overlapping orbitals. This angular dependence is essentially determined by integration of various combinations of spherical harmonics with respect to angle.

The problem of tunneling, taking into account the mutual influence of the tip and crystal on the spectrum, also admits an elegant solution within the tight-binding method. This problem was solved in the paper by Caroli *et al.*,¹⁵ using the nonequilibrium techniques of Keldysh¹⁴ in the one-dimensional case and for one type of orbital at each lattice site.

Let us obtain an expression for the tunneling current in our case, and show that when the mutual influence of the tip and crystal is neglected (to lowest order in the tunneling matrix element), the problem reduces to the Bardeen-Tersoff-Hamann form.¹ We emphasize that this approach includes the change in the tip and crystal spectrum due to the overlap of their orbitals, but does not take into account a possible shift of the atoms at the surface when the tip is applied.

In what follows, it is convenient to treat the crystal and tip as two clusters of finite but rather large numbers of atoms that are periodically repeated along the surface. The Hamiltonian of the noninteracting tip and crystal can be written in the form

$$\hat{H}_{c,t} = \sum_{i,j} \sum_{c,t} \varepsilon_{in} c_{i\sigma}^+ c_{j\sigma} + \sum_{i,j} \sum_{c,t} [T_{nn'}^{ij} c_{i\sigma}^+ c_{jn'\sigma} + \text{h.c.}], \quad (4)$$

where the labels c, t refer to the crystal and tip, respectively, and σ is a spin index. The overlap integral is denoted by the same letters as in Eq. (1), according to a principle that will become clear in what follows. In determining it we find

$$T_{nn'}^{ij} = \langle \varphi_{nc}(\mathbf{r}-\mathbf{R}_i) | \hat{T} | \varphi_{n't}(\mathbf{r}-\mathbf{R}_j) \rangle, \quad (5)$$

where \hat{T} is an "overlap" operator whose form will be made more precise below; $\varphi_{nc}(\mathbf{r}-\mathbf{R}_i)$ are n -type orbitals ($n = s, p, d, \dots$) centered on atom \mathbf{R}_i in the crystal (label c) or in the tip (label t). In Eq. (4), ε_{in} has the sense of an energy eigenvalue for an electron on an isolated n -type orbital at the position \mathbf{R}_i .

Tunneling between the crystal and the tip is possible due to the overlapping orbitals. In this case, the tunneling Hamiltonian has the form

$$\hat{T} = \sum_{i,j} \sum_{n,n',\sigma} [T_{nn'}^{ij} c_{i\sigma}^+ c_{jn'\sigma} + \text{h.c.}], \quad (6)$$

Due to the rapid decay of the value of the matrix element $T_{nn'}^{ij}$ with distance, the important contribution to \hat{T} comes from orbitals for the sharp point and the regions of the surface close to it. The tunneling current between the two subsystems is determined by the expression

$$I = \langle \hat{I} \rangle = e \left\langle \frac{d\hat{N}_c}{dt} \right\rangle = i\hbar \langle [\hat{N}_c, (\hat{H}_c + \hat{H}_t + \hat{T})] \rangle, \quad (7)$$

where the current operator has the form

$$\hat{I} = \frac{ie}{\hbar} \sum_{i,j} \sum_{n,n',\sigma} [T_{nn'}^{ij} c_{i\sigma}^+ c_{jn'\sigma} - \text{h.c.}]. \quad (8)$$

In what follows, it is convenient to go over to matrix form in the description, introducing the notation

$$\hat{T} = \{T_{nn'}^{ij}\}, \quad \hat{C}_{c,t} = \{c_{c,ijn\sigma}\}. \quad (9)$$

Taking into account Eqs. (7)–(9), we find

$$I = ie \text{Sp} \{ \hat{T} \langle \hat{C}_c^+(t) \hat{C}_t(t) \rangle - \langle \hat{C}_t^+(t) \hat{C}_c(t) \rangle \hat{T}^+ \} = e \text{Sp} \{ \hat{T} \hat{G}_{ct}^{+-}(t, t) - \hat{G}_{tc}^{+-}(t, t) \hat{T}^+ \}, \quad (10)$$

the trace operation Sp in Eq. (10) is calculated after matrix multiplication with respect to all the orbitals and spatial labels of these orbitals, and the Keldysh functions are defined in the usual way as follows:

$$\hat{G}_{ct}^{+-}(t, t') = i \langle \hat{C}_c^+(t) \hat{C}_t(t') \rangle, \quad (11)$$

$$\hat{G}_{tc}^{+-}(t, t') = i \langle \hat{C}_t^+(t) \hat{C}_c(t') \rangle. \quad (12)$$

The expression for the tunneling current (10) is valid to any order in the tunneling matrix elements of \hat{T} , and can be converted to the form

$$I = \frac{2\pi e}{\hbar} \int \frac{d\varepsilon}{(2\pi)^2} \times \text{Sp} \left\{ \frac{\hat{T} \hat{g}_{cc}^-(\varepsilon) \hat{T}^+ \hat{g}_{tt}^+(\varepsilon) - \hat{T}^+ \hat{g}_{tt}^-(\varepsilon) \hat{T} \hat{g}_{cc}^+(\varepsilon)}{|\text{Det}(\varepsilon)|^2} \right\}, \quad (13)$$

where $\hat{g}_{cc,tt}^{\pm}(\varepsilon)$ are Keldysh functions (the caret denotes a matrix with respect to the orbital labels) for the noninteracting crystal and tip, respectively. We also introduce the notation

$$|\text{Det}(\varepsilon)|^2 = \text{Det}^R(\varepsilon) \text{Det}^A(\varepsilon), \quad (14)$$

$$\text{Det}^{R,A}(\varepsilon) = \det \begin{pmatrix} \hat{I}, \hat{T} \hat{g}_{cc}^{R,A}(\varepsilon) \\ \hat{T}^+ \hat{g}_{tt}^{R,A}(\varepsilon), \hat{I} \end{pmatrix},$$

where $\hat{g}^{R,A}(\varepsilon)$ are the retarded and advanced Green's functions, and \hat{I} is the unit matrix of corresponding dimension. We assume that the applied voltage is included in the distribution functions, which are contained in $\hat{g}_{cc,tt}^{\pm}(\varepsilon)$. Making use of the relation

$$\hat{g}_{cc,tt}^{\pm}(\varepsilon) = 2\pi i \hat{\rho}_{c,t}(\varepsilon) \begin{cases} n_{c,t}(\varepsilon) \\ n_{c,t}(\varepsilon) - 1 \end{cases}, \quad (15)$$

where $\hat{\rho}_{c,t}(\varepsilon)$ are the density-of-states matrices of the crystal and tip, and $n_{c,t}(\varepsilon)$ is the Fermi distribution function

$$\hat{\rho}_{c,t}(\varepsilon) = -\frac{1}{\pi} \text{Im} \{ \hat{g}_{cc,tt}^R(\varepsilon) \}, \quad (16)$$

Eq. (13) can be simplified, and the expression for the tunneling current, valid for any tunnel coupling between tip and crystal finally takes the form

$$I = \frac{2\pi e}{\hbar} \int d\varepsilon \text{Sp} \left\{ \frac{\hat{T} \hat{\rho}_c(\varepsilon) \hat{T}^+ \hat{\rho}_t(\varepsilon)}{|\text{Det}(\varepsilon)|^2} \right\} [n_c(\varepsilon) - n_t(\varepsilon - eV)], \quad (17)$$

where V is the external applied voltage.

We note that in the weak tunnel coupling limit (i.e., large distance between tip and surface), we can assume that $|\text{Det}(\varepsilon)|^2$ in Eq. (17) is ~ 1 to terms $\sim T^2$. Let us show that in this limit Eq. (17) reduces to the Bardeen-Tersoff-Hamann equation (1).

Before doing this, we note that according to the paper by Goldberg *et al.*,¹⁶ under rather general assumptions the hopping integral (5) (see Ref. 16 for details) reduces to the following expression within the tight-binding method:

$$T_{nn'}^{ij} = \frac{\hbar^2}{2m} \int ds (\varphi_{nc}(\mathbf{r}-\mathbf{R}_i) \nabla \varphi_{n't}(\mathbf{r}-\mathbf{R}_j) - \varphi_{n't}(\mathbf{r}-\mathbf{R}_j) \nabla \varphi_{nc}(\mathbf{r}-\mathbf{R}_i)), \quad (18)$$

which agrees with the tunneling matrix element of Bardeen⁶ [Eq. (2)]. This agreement is not surprising if we recall that electron hopping between atoms takes place via the same tunnel coupling between two adjacent potential wells (the potentials of which can be replaced by pseudopotentials).

We now find the density of states matrix $\hat{\rho}_{c,t}$. For convenience, we let the label k denote the pair of indices n,i , and $\varphi_{nc}(\mathbf{r}-\mathbf{R}_i) = |\varphi_k\rangle$. The wave eigenfunction of energy level ε_μ (tip or crystal) $|\Psi_\mu\rangle$ can be expanded in terms of the localized orbitals $|\varphi_k\rangle$:

$$|\Psi_\mu\rangle = U_{\mu k} |\varphi_k\rangle, \quad (19)$$

where $U_{\mu k}$ is a matrix of expansion coefficients, and $|\Psi_\mu\rangle$ and $|\varphi_k\rangle$ are columns with dimensions $\{N_A \times N_O\}$ (N_A is the number of atoms, N_O the number of orbitals per atom). In the basis of the eigenfunctions of the Hamiltonian, the Green's function has the simple form

$$\hat{g}^R(\varepsilon) = \sum_{\mu} \frac{|\Psi_\mu\rangle \langle \Psi_\mu|}{\varepsilon - \varepsilon_\mu + i0}, \quad (20)$$

$$\hat{\rho}(\varepsilon) = -\frac{1}{\pi} \text{Im} \{ \hat{g}^R(\varepsilon) \} = \sum_{\mu} |\Psi_\mu\rangle \langle \Psi_\mu| \delta(\varepsilon - \varepsilon_\mu). \quad (21)$$

Completing the transition in (21) to a basis of localized orbitals using (19), we have

$$\hat{\rho}(\varepsilon) = \sum_{\mu, k, k'} U_{k'\mu}^+ U_{\mu k} |\varphi_k\rangle \langle \varphi_{k'}|, \quad (22)$$

taking into account Eqs. (5), (17), and (22), we find to within terms of order T^2

$$I = \frac{2\pi e}{\hbar} \sum_{\substack{k, k' \\ l, m \\ \nu, \mu}} \{ \langle \varphi_{lk} | \hat{T} | \varphi_{ch'} \rangle (U_{k'\mu}^+ U_{\mu l}) \langle \varphi_{ll} | \hat{T} | \varphi_{cm} \rangle (U_{m\nu}^+ U_{\nu l}) \times \delta(\varepsilon_\nu - \varepsilon_\mu) \} [n(\varepsilon_\nu) - n(\varepsilon_\mu)]. \quad (23)$$

Using Eq. (19), we finally obtain

$$I = \frac{2\pi e}{\hbar} \sum_{\nu, \nu'} |T_{\nu\nu'}|^2 \delta(\varepsilon_\nu - \varepsilon_{\nu'}) [n(\varepsilon_\nu) - n(\varepsilon_{\nu'})], \quad (24)$$

which coincides with Eq. (1).

The tight-binding method is most convenient for calculating spectra and other properties of systems that do not possess translation invariance. This is the situation for STM modeling. In practical calculations based on empirical tight binding there is no need to explicitly use orbitals to construct the Hamiltonian: it is sufficient to know only the geometric placement of the atoms and the types (symmetry) of orbitals at each site. After this the Hamiltonian can be written explicitly in the form of a matrix.

Unfortunately, direct computation using Eq. (17) requires knowledge of the matrix of expansion coefficients with respect to localized orbitals. In these calculations it is necessary to know not only the spectrum (eigenvalues) of the Hamiltonians of the tip and crystal, but also their eigenvectors. Finding the latter requires large computational resources.

However, as was shown in Refs. 17 and 18, the tunneling current can be calculated without finding the eigenvectors. In this case, the problem reduces to finding the complex energy spectrum of the composite cluster tip + crystal, in which case their mutual influence is taken into account automatically. In the next section this approach will be applied to modeling STM images on the (110) surface of GaAs.

3. MODELING STM IMAGES OF THE (110) SURFACE OF GaAs

The cleaved (110) surface of GaAs, along with the (111) Si 2×1 , (111) Si 7×7 , and graphite surfaces, have received the most study, both by STM¹⁹⁻²¹ and by other techniques.²² The atomic structure of an ideal (110) GaAs surface shown in Fig. 1a turns out to be unstable and undergoes relaxation (Fig. 1b). That the (110) GaAs surface has the structure shown in Fig. 1b is now considered to be reliably established. For this surface there are a variety of calculations based on minimum energy (see Ref. 23 and the citations therein), which give roughly the same values for the relaxation parameters. In this paper we use the relaxation parameters and matrix elements of the tight-binding Hamiltonian obtained by Chadi.²³ The total electron density of states in the upper layer of a relaxed surface and the partial density of states on individual orbitals of Ga and As atoms in this case are shown in Figs. 2a to 2c. For an ideal surface there are two bands of surface states in the gap for the bulk density of states, one of which is formed essentially by atomic Ga states, the other by As states; during relaxation these two bands are expelled into the bulk conduction and valence bands, respectively.^{24,25} Our calculations of the density of states are in rather good agreement with those of other authors (see, e.g., Refs. 24,25).

The tip is modeled as a linear chain of 20 atoms placed perpendicular to the plane of an ideal surface. At each atom

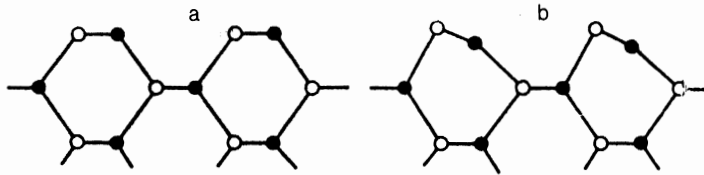


FIG. 1. Side view [(projection on the plane (110))] of the (110) surface of GaAs. The filled circles are Ga atoms, the open circles As; a—ideal surface, b—relaxed surface.

we have centered one s -type orbital with a single electron. The value of the overlap integral in the chain was chosen to equal 1 eV. The crystal was modeled as a periodically repeating cluster consisting of 2×2 unit cells in the plane of the surface with a thickness of 8 atomic layers; in the calculations we took into account the interaction of the last atom of the tip with all the atoms in the first crystal layer. The over-

lap integrals between orbitals localized on tip and crystal atoms were chosen in the following way:

$$(s|s) = f(d), \quad (s|p_x) = f(d)l, \quad (s|p_y) = f(d)m, \quad (s|p_z) = f(d)n, \quad (25)$$

$$f(d) = \exp[-(d-1)], \quad (26)$$

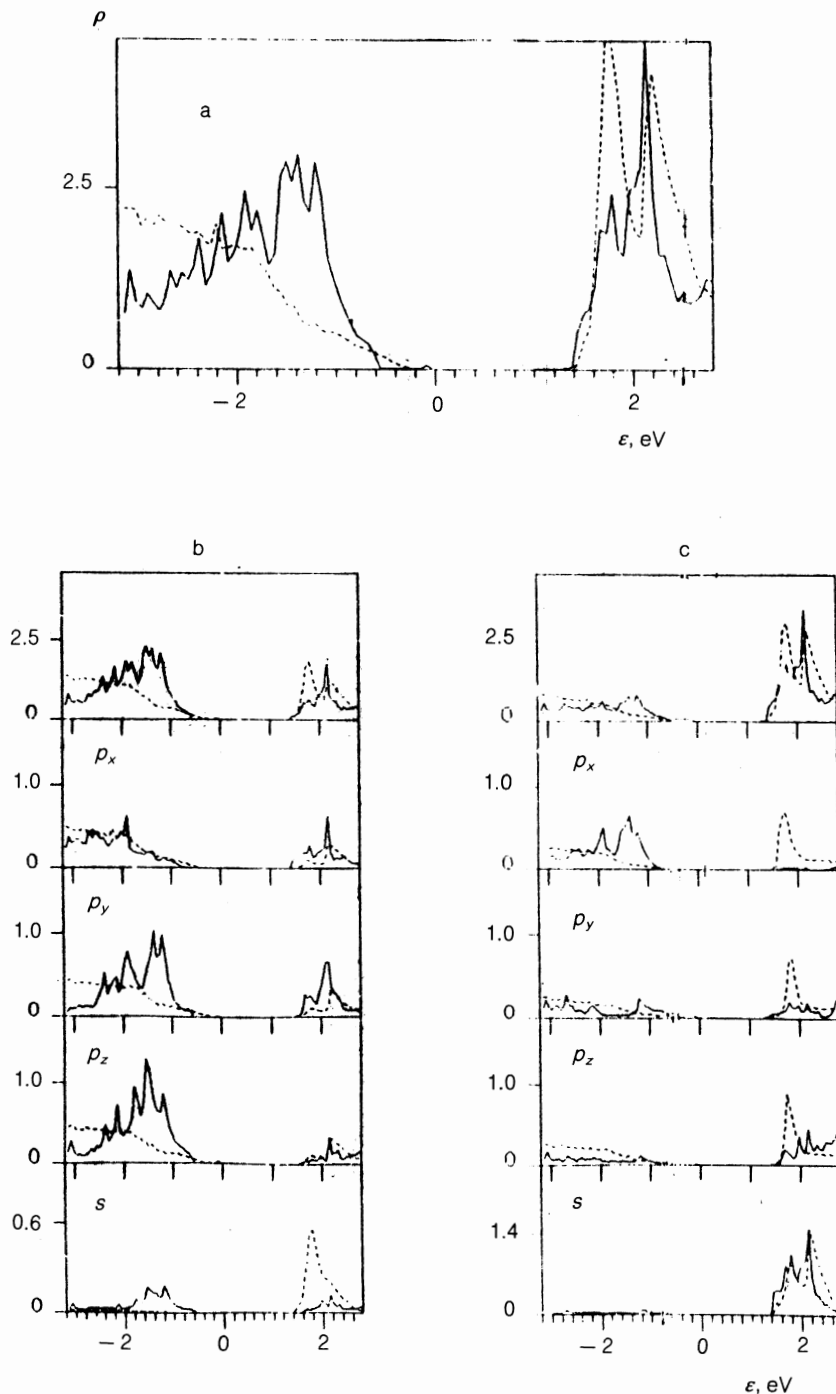


FIG. 2. a—total density of states in the upper layer of a relaxed (110) GaAs surface. The partial densities of states at individual orbitals are shown for As atoms (b) and Ga atoms (c): the solid curves refer to the surface, the dashed curves to the bulk.

where l, m, n are direction cosines between the directions of the "dumbbell"-shaped p_i orbitals and the radius vector that connects atoms of the tip and crystal, and d is the interatomic spacing in angstroms. The dependence of the matrix elements (25) on distance through (26) is essentially determined by the work function, which for the majority of solids has a value on the order of 4 to 5 eV; this agrees with the data from the tables of Clementy and Roetty.²⁶ In fact, the qualitative character of this dependence leads to considerable indeterminacy in the value of the tunneling current. Direct comparison of the absolute value of the tunneling current for a specific experiment, when the tip is positioned above a specific point, is made still more difficult by the fact that the tunneling current, as we have already noted previously, depends on the atomic structure of the sharp point. However, this does not imply that such a comparison is impossible. In fact, methods have recently been developed for obtaining tips with known point geometries. Reference 27 report fabricating a tungsten tip with a pyramid made up of four atoms at its point. The presence of the pyramid was clearly demon-

strated using an ion microscope; furthermore, it is clear from Ref. 27 that the procedure for obtaining such a tip is quite reproducible. If the shape of the sharp point is known, then calculations are possible for any specific situation. Nevertheless, use of a simple linear tip and matrix overlap elements determined by Eqs. (25) and (26) is found to be sufficient for a good qualitative description of the experimental results.

In Figs. 3a, 3b and 4a, 4b we show STM images of a relaxed (110) GaAs surface calculated in the constant current regime ($|I| = 0.1$ nA) when voltages $U = +2$ V and -2 V were applied to the crystal, respectively. The energies of the atomic orbitals in the tip were chosen so that the Fermi levels in the crystal and tip coincided in the absence of an applied voltage. In the first case ($U = +2$ V), electrons tunnel from the tip into the conduction band of the crystal, which was formed essentially from s -type orbitals of Ga (Fig. 2b). When $U = -2$ V, the valence electrons of the crystal participated in the tunneling; these electrons are localized primarily in p -orbitals of the As atoms (Fig. 2c). In

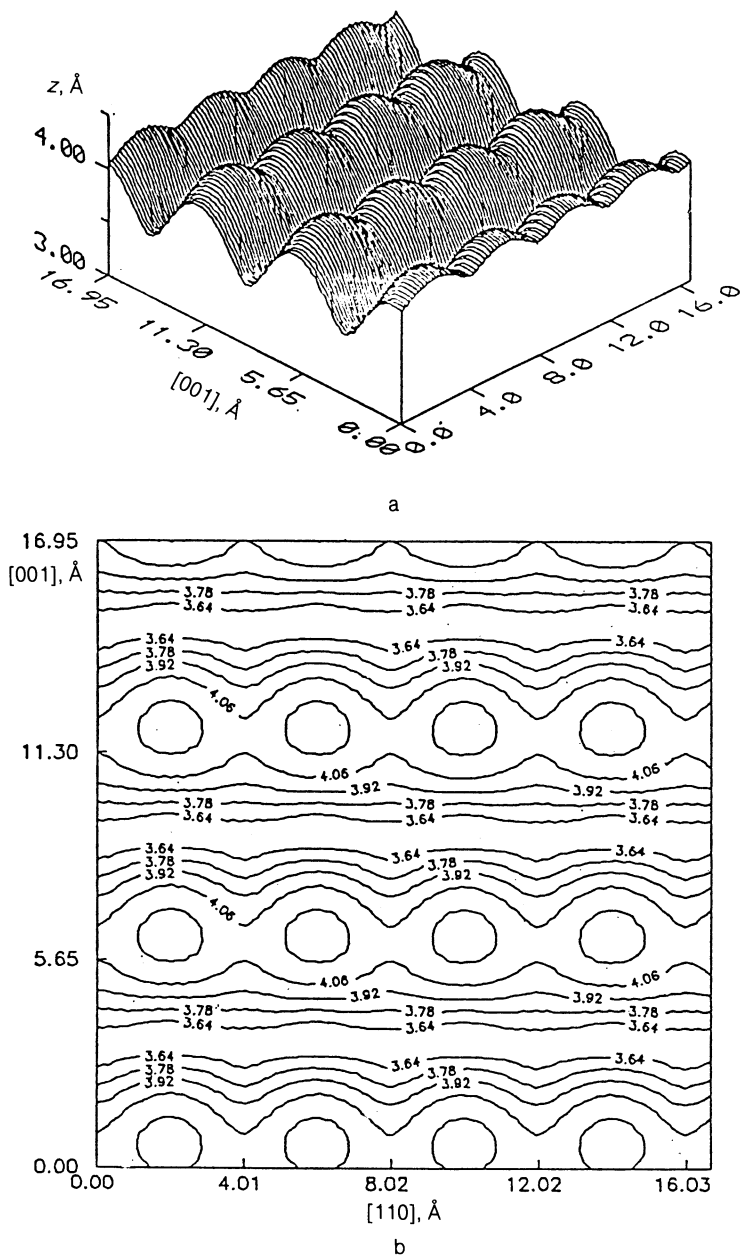


FIG. 3. a—three-dimensional image of the profile of a (110) GaAs surface, calculated in the constant-current regime ($I = 0.1$ nA) with a voltage $U = 2$ V applied to the crystal. b—topographical image of this profile. The coordinate origin coincides with the position of an As atom on an ideal surface. The distance along the z -axis is measured from the tip atom closest to the crystal to the plane of the ideal surface.

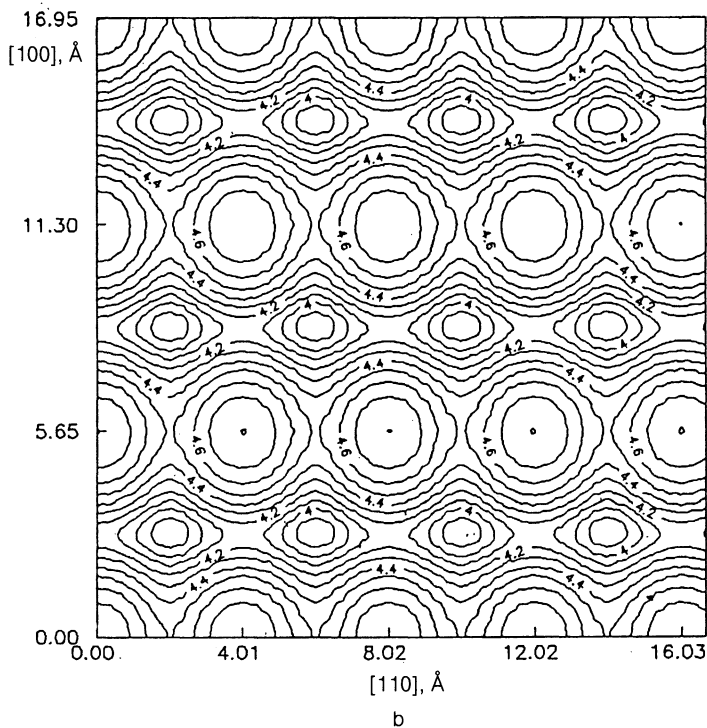
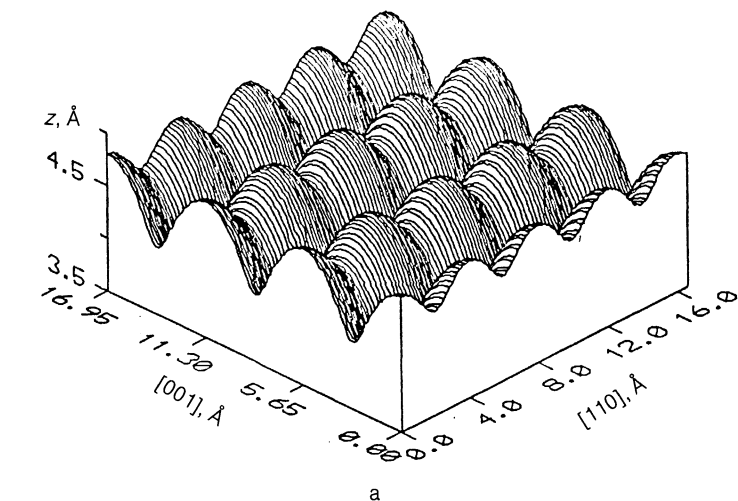


FIG. 4. The same as in Fig. 3, but for a voltage $U = -2$ V applied to the crystal.

agreement with this, the bumps in the STM image (Fig. 3a) corresponded to Ga atoms for $U = 2$ V, and atoms of As were not observed. Conversely, when the sign of the voltage was changed, an image of the As atoms appeared (the bumps in Fig. 4a), and the Ga atoms dropped out of the picture.

From Figs. 3a and 4a it is clear that in both cases the modulation of the distance from the sharp point to the surface was much larger in the [001] direction than in the [110] direction. All of these results are in complete agreement with experiment;^{19,20} however, it should be noted that the spacings in the [001] direction observed in Ref. 19 between maxima in the profile of the STM images (corresponding to atoms of Ga and As) obtained for $U = \pm 1.9$ V were found to equal 1.8 \AA (an average over various series of measurements gives $2.1 \pm 0.09 \text{ \AA}$), while in our calculations they are practically indistinguishable from the spacings in the [001] direction between atoms of Ga and As in the uppermost layer of the relaxed surface (approximately 1.25 \AA). At this time the reason for this considerable disagree-

ment between theory and experiment is unclear.

The comparison of experimental and theoretical STM images given in Ref. 19 (the latter calculated using the Tersoff-Hamann method) gives better agreement with experiment, although the calculations do not take into account the mutual influence of the tip and crystal. Our calculations, which do take into account the mutual effect of the tip and crystal on their electronic spectra, show that it is impossible to achieve complete agreement with experiment. Both our calculations were made for a fixed surface geometry. However, when a voltage is applied and an excess charge (or deficit) appears, it is possible for the surface to distort compared to a free surface during the tunneling of electrons from the bond to the surface. Thus, in STM experiments involving the Si (001) 2×1 surface one often observes symmetric dimers, whereas other experiments and theoretical calculations of the free reconstructed surface indicate that an asymmetric-dimer model is appropriate (see the detailed analysis of data in the paper by Badziag²⁸). An attempt has been

made²⁸ to explain this contradiction by taking into account the distortion that accompanies the charging of these dimers while electrons are tunneling. We note that the change in the geometry of adsorbed molecules of CO type during scanning by a tip along a surface can turn out to be significant in the interpretation of STM images (see discussion in the paper by Stoneham *et al.*²⁹). We cannot exclude the possibility that atomic relaxation on the surface during electron tunneling can occur for the (110) surface of GaAs as well.

Thus, the use of the method of quasistationary states to calculate the tunneling current within the framework of a simple tight binding model leads to a good qualitative description of STM images. As for quantitative comparisons with experiment, for this we apparently require inclusion of the real atomic structure of the sharp point and a more accurate calculation of the overlap matrix elements between tip and crystal orbitals, and possibly the inclusion of surface relaxation during the electron tunneling.

- ¹G. Binnig, H. Rohrer, C. Gerber, and E. Weibel, *Phys. Rev. Lett.* **49**, 57 (1982).
²G. Binnig and H. Rohrer, *Helv. Phys. Acta* **55**, 726 (1982).
³G. Binnig and H. Rohrer, *IBM J. Res. Devel.* **30**, 355 (1986).
⁴G. Binnig and H. Rohrer, *Surf. Sci.* **152/153**, 17 (1985).
⁵P. K. Hansma and J. Tersoff, *J. Appl. Phys.* **61**, R1 (1987).
⁶J. Bardeen, *Phys. Rev. Lett.* **6**, 57 (1961).
⁷J. Tersoff and D. R. Hamann, *Phys. Rev. Lett.* **50**, 1998 (1982); *Phys. Rev. B* **31**, 805 (1985).
⁸A. Baratoff, *Physica B* **127**, 143 (1984).
⁹C. J. Chen, *Phys. Rev. Lett.* **65**, 448 (1990).

- ¹⁰C. J. Chen, *Phys. Rev. B* **42**, 8841 (1990).
¹¹J. Tersoff, *Phys. Rev. B* **41**, 1235 (1990).
¹²E. Tekman and S. Ciraci, *Phys. Rev. B* **40**, 10286 (1989).
¹³W. A. Harrison, *Electronic Structure and the Properties of Solids*. San Francisco: Freeman Publ., 1980.
¹⁴L. V. Keldysh, *Zh. Eksp. Teor. Fiz.* **47**, 1515 (1964) [*Sov. Phys. JETP* **20**, 1018 (1965)].
¹⁵C. Caroli, R. Combescot, P. Nozières, and D. Saint-James, *J. Phys. C* **4**, 916 (1971).
¹⁶E. C. Goldberg, A. Martin-Rodero, R. Monreal, and F. Flores, *Phys. Rev. B* **39**, 5684 (1988).
¹⁷S. V. Meshkov and S. N. Molotkov, *Zh. Eksp. Teor. Fiz.* **100**, 1640 (1991) [*Sov. Phys. JETP* **73**, 906 (1991)].
¹⁸S. N. Molotkov, S. S. Nazin, I. S. Smirnova, and V. V. Tatarskiĭ, *Surf. Sci.* **259**, 339 (1991).
¹⁹J. Tersoff, R. M. Feenstra, J. A. Stroscio, and A. P. Fein, *J. Vac. Sci. Technol. A* **6**, 497 (1988).
²⁰J. A. Stroscio, R. M. Feenstra, D. M. Newns, and A. P. Fein, *J. Vac. Sci. Technol. A* **6**, 499 (1988).
²¹R. M. Feenstra, *Interaction of Atoms and Molecules with Solid Surfaces*, p. 357, V. Bortolani *et al.*, eds., Plenum Publ., New York, 1990.
²²L. Smit, T. E. Derry, and J. F. van der Veen, *Surf. Sci.* **150**, 245 (1985).
²³D. J. Chadi, *Phys. Rev. B* **19**, 2074 (1979).
²⁴W. A. Goddard, J. J. Barton, A. Redondo, and T. C. McGill, *J. Vac. Sci. Technol.* **15**, 1274 (1978).
²⁵J. R. Chelcovsky and M. L. Cohen, *Solid State Commun.* **29**, 267 (1979).
²⁶E. Clementy and R. Roetty, *Atom. Data and Nucl. Tables* **14**, 177 (1974).
²⁷H.-W. Fink, *Phys. Scripta* **38**, 260 (1987).
²⁸P. Badziag, W. S. Verwoed, and M. A. van Hove, *Phys. Rev. B* **43**, 2058 (1991).
²⁹M. Ramos, A. P. Sutton, and A. M. Stoneham, *J. Phys. Condensed Matter* **3**, S127 (1991).

Translated by Frank J. Crowne